Detection of gaseous plumes in airborne hyperspectral imagery

Eyal Agassi[a], Eitan Hirsch[a], Martin Chamberland[b], Marc-André Gagnon[b], Holger Eichstaedt[c]

[a]Environmental Physics Department, Israel Institute for Biological Research, P.O.Box 19, Nes Ziona Israel; [b]Telops Inc, 100-2600 St-Jean-Baptiste avenue, Québec, QC, Canada G2E 6J5; [c]Dimap HK Pty Ltd, 32F, Millennium City 1, 388 Kwun Tong Road. Kowloon, Hong Kong S.A.R.

ABSTRACT

The thermal hyperspectral sensor Hyper-Cam was mounted on a light aircraft and measured continuous releases of several atmospheric tracers from a height of 2 km. A unique detection algorithm that eliminates the need for clear background estimation was operated over the acquired data with excellent detection results. The data-cubes were acquired in a "target mode", which is a unique method of operation of the Hyper-Cam sensor. This method provides multiple views of the plume which can be exploited to enhance the detection performance. These encouraging results demonstrate the utility of airborne LWIR hyperspectral imaging for efficient detection and mapping of effluent gases for environmental monitoring.

Keywords: hyperspectral, LWIR, airborne, gas plume, detection

Chemical, Biological, Radiological, Nuclear, and Explosives (CBRNE) Sensing XVII, edited by Augustus Way Fountain III, Proc. of SPIE Vol. 9824, 98240U · © 2016 SPIE · CCC code: 0277-786X/16/$18 · doi: 10.1117/12.2222142

1. INTRODUCTION

FTIR technology has been widely used for the remote detection and identification of gas plumes. In 2005, when Telops introduced the Hyper-Cam, the first commercial hyperspectral imager operating in the thermal infrared band, imaging and tracking of gas plumes was demonstrated. Since then, many R&D groups developed algorithms and data processing capabilities to convert the hypercubes of radiance obtained with the Hyper-Cam into real-time videos of gas plumes. IIBR scientists refined the gas imaging algorithms further to include an essential capability, the in-scene automatic background determination. With this powerful algorithm, there is no need to have a measurement of the background prior to a gas release, enabling the possibility to detect and identify gas clouds from airborne measurements. In this paper, after an introduction to the airborne Hyper-Cam, we present the experimental setup we used to validate the detection of gaseous plumes from airborne hyperspectral imagery. The algorithms are briefly described and data analysis of airborne measurements is performed. Images of detection results are presented showing the performance of the solution.

2. AIRBORNE HYPER-CAM

The Hyper-Cam is a lightweight and compact imaging spectrometer. It has been introduced as a commercial product by Telops in 2005 [1] and has been widely used by several groups to demonstrate a great number of applications [2-7]. A picture of the Hyper-Cam is shown in Figure 1 . The Hyper-Cam used for the work presented here is a LWIR, covering the infrared band from 7.8µm to 11.8µm. Its Focal Plane Array (FPA) is a cooled MCT with 320×256 pixels. The spectral resolution is user selectable from 0.25cm^{-1} to 150cm^{-1}. The basic field of view is 6.4°×5.1° which can be modified with the use of an afocal telescope. Compatible with the airborne configuration, there is a 0.25× telescope providing a total field of view of 25.6°×20.4° where each pixel has an IFOV of 1.4mrad. For the experiment of this paper, we used the basic configuration, so each pixel has an IFOV of 350µrad.

Figure 1: Picture of the Hyper-Cam.

The airborne configuration of the Hyper-Cam is a clever approach where the same optical head used for ground-based measurements just needs to be installed on a dedicated stabilizing platform. The platform, presented in Figure 2, is equipped with a 2-axis pointing mirror for active image stabilization. It also has a GPS/INS unit for an accurate geolocation of each measurement.

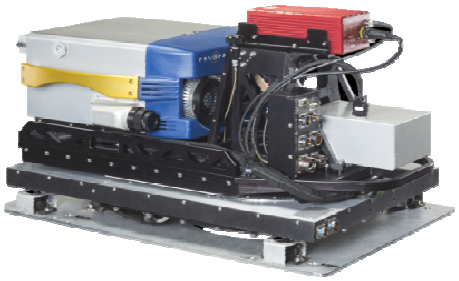

Figure 2 –Hyper-Cam installed on the stabilization platform for airborne operations.

The airborne Hyper-Cam offers two modes of operation as illustrated in Figure 3. The first one is named the mapping mode, where each hypercube slightly overlaps with the preceding one resulting in a 100% coverage of the ground. Complete maps can be produced by stitching these hypercubes.

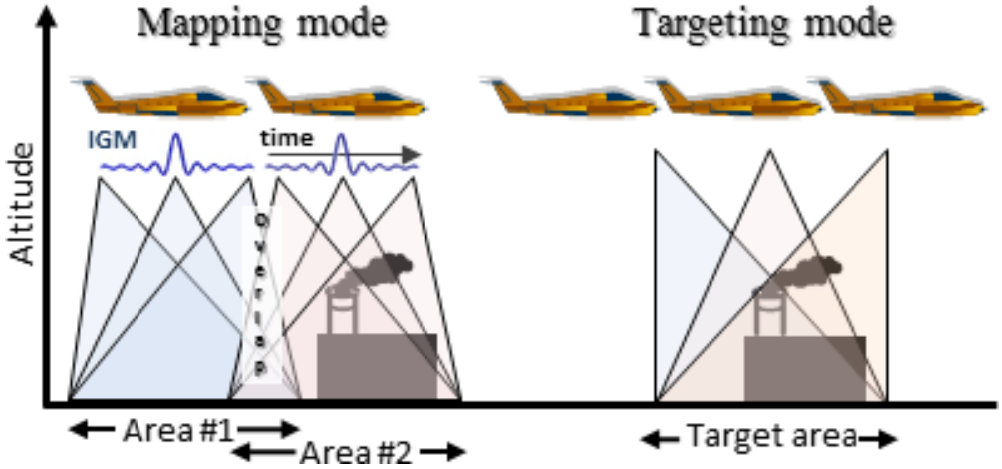

Figure 3 –The 2 operating modes offered by the airborne Hyper-Cam.

The second mode is the targeting mode. In this mode, unique to the Hyper-Cam, several hypercubes are acquired over a selected ground target, through a GPS coordinate, as far as the tracking range of the image motion compensation mirror allows. Hypercubes acquired in that mode can be averaged to increase the SNR or used to determine temporal variations of the scene. The airborne Hyper-Cam produces high quality radiance hypercubes, same as when operated ground-based, allowing gas detection and identification to be achieved.

3. EXPERIMENTAL

A small scale field test was conducted to prove the feasibility of detection and identification of gaseous plumes using airborne hyperspectral imaging. The experimental setup was composed from three elements:

1. Installing the hyperspectral sensor (HyperCam, Telops Inc., Canada) on a light aircraft, operating and data gathering during the flight, calibrating the acquired data and delivery of the data-cubes to the user for analysis: Dimap (HK).
2. Operating the light aircraft (Piper Navaho) during the campaign: Ofek Air Ltd (Israel).
3. Ground release of atmospheric tracers and meteorological measurements: IIBR (Israel).

The sensor and its components were installed on the aircrafts on the ground (see Figure 4).

Figure 4 – Onboard installation of HyperCam sensor on the light aircraft. Left and right – Sensor installation inside the aircrafts; Middle-down – a view from below; Middle-up – a general view of the aircraft.

Figure 5 – Ground setup at release point. Left – on site meteorological station; Middle-down – release point; Middle-up – mass flow controllers; Right – release stack.

The flight parameters were set using Telops' software Flight Assistant which optimizes the best sensor performance according to the desired flight profile. The main constraints on the flight parameters were the spectral resolution ($4cm^{-1}$) and FOV optics (5X6°), minimum image size and aircraft speed. Also, since the exact location of the release point was known – we operated the sensor at a target mode. The combination of all of these constrains yielded a flight height of 2km and provided between 1-2 datacubes at each pass over the release point.

The ground release point was located in a middle of a planar and open rural area. The dissemination was carried out from an original high pressure cylinder through mass flow controller in order to ensure constant flow of 2 Kg/min of each atmospheric tracer (SF_6, CHF_3, and R134a) through a stack (3m high, 40cm in diameter and air flow of 10000 m^3/hour). A 2m meteorological mast was mounted near the release point to provide the air velocity, air temperature and its humidity. A total of 9 successful passes over the release point were carried out – 3 releases of each tracer. Every release was synchronized with data acquisition using air to ground communication link in order to ensure that the obtained datacube will include a fully developed plume. The measurement was conducted around noon time. The weather was very typical to this area during the summer: mostly sunny, warm and somewhat humid (28.5˚C, RH of 50%) and a prevailing sea breeze (2-3 m/s from northwest). Figure 5 shows the ground setup. Upon aircraft landing, the raw data were calibrated and handed for processing.

4. DATA ANALYSIS

As mentioned before, the main objective of the airborne measurement campaign was to prove that a previously developed algorithm aimed to detect and identify gaseous plumes from ground based

hyperspectral imaging is also applicable for airborne operation without substantial modifications. The detection and identification algorithm had been widely described in previous publications [10-11] and we will briefly survey it again. The algorithm has two successive steps:

The first step is spatial-spectral hierarchical unsupervised clustering based on the 3D content of a single data-cube. It is carried out by top-down K-means clustering with a correlation metrics at the spectral domain. The clustering procedure is halted when the size of a cluster falls below preset criterion. At the end of this process, the datacube is decomposed into a typical number of 2000-3000 clusters (scene content depended). Each cluster is characterized by a spatial connectivity and high mutual spectral correlation between all its elements. This step is the most fundamental of the algorithm and requires high quality hyperspectral imagery at a spectral resolution of about $4cm^{-1}$ that cannot be degraded.

The next step uses a physical model of gas plume radiative transfer is order to identify the target gas and to extract it location.

$$\tau_g = \frac{T_s - T_{air}}{T_{bgd} - T_{air}} \tag{1}$$

Each cluster is used twice: first as T_s where all the others are used as potential clear backgrounds, and second as a T_{bgd} for all the other pixels. The correlation coefficient between the obtained transmissions and those of the target gases is calculated and if it passed predefined threshold – the cluster is assigned as a part of the target gas plume that is obtained by the union of all the other yielded clusters. It is assumed that a minimum size of a cluster must be over 50 pixels in order to avoid false detections. The algorithm is insensitive to atmospheric transmission (as long signal to noise ratio remains adequate), but it is very sensitive to insufficient spectral resolution. Therefore, we have decided to acquire the hyperspectral imagery at high spectral resolution, even when it determinates a cruise altitude of 2 km (A narrow field of view and a target mode were preferred in order to acquire large portion of the plume). When an airborne imagery is used as an input for the detection algorithm, no change is expected in the results of the clustering phase. However, there is a fundamental difference in the signal formation radiative transfer equations. At a horizontal path, the air temperature and the atmospheric attenuation coefficient are constant throughout the path. This is not the case at airborne imaging when they are both a function of the altitude.

It can be shown that at airborne imaging eq. 2 is modified into:

$$\tau_g = \frac{T_s - \left\lfloor T_{a(0)} \cdot \tau_a + path \right\rfloor}{\left\lceil T_{bgd}\tau_a + path \right\rceil - \left\lceil T_{a(0)} \cdot \tau_a + path \right\rceil} \tag{2}$$

As in equation 1, T_s and $T_{bgd}\tau_a + path$ are direct measurements, but now the estimation of $T_{a(0)} \cdot \tau_a + path$ is required instead of T_{air}. It is a much harder task since it requires to know both the air temperature at the plume plane and the atmospheric temperature and humidity profile. Ground meteorological station is a partial solution but not complete one as it provides only ground level data and additional estimation is needed. It can be achieved via atmospheric transmission and radiance models such as MODTRAN or through any other models based on the obtained data cube that exploit its high spectral resolution and the known boundary conditions to provide a good estimate of the temperature and humidity profiles. At the current stage, we guess the quantity $T_{a(0)} \cdot \tau_a + path$ through the analysis of the best obtained detection results, but this issue has to be settled in the future in order to allow a practical use.

Some results are shown in next figures after a visible image of the scene which presented at Figure 6.

Figure 6 – A visible image of the scene (acquired by HyperCam visible camera) from a height of 2km. The release point is marked by a black circle.

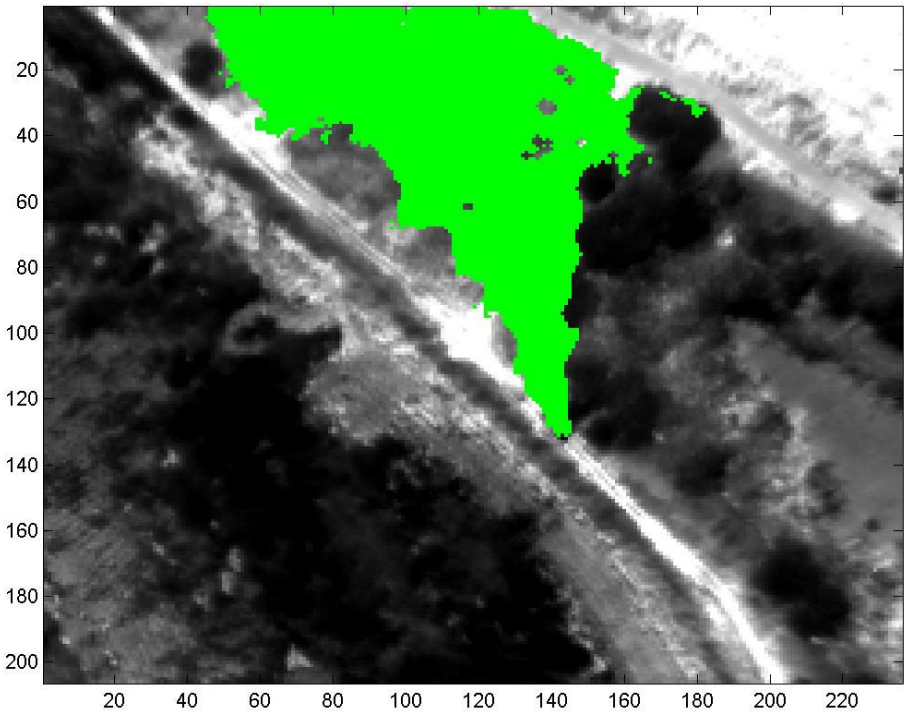

Figure 7 – Detection results – an SF_6 plume.

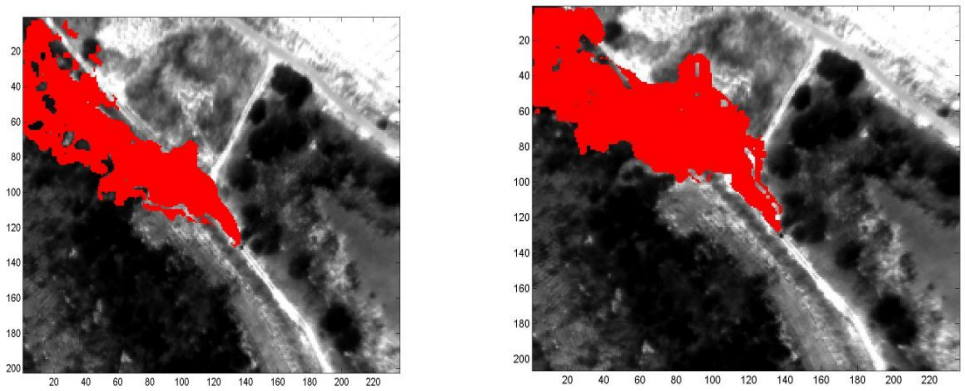

Figure 8 – Detection results – CHF_3 plume. Two consecutive datacubes at the same pass.

The detection results were very good: the structure of the plume is clearly visible and with no false detection. Therefore, we can adopt the algorithm performance as quoted in a previous publication [10] for the airborne imaging as well. It significantly enhances the utility of this specific algorithm and proves again its robustness.

5. SUMMARY AND CONCLUSIONS

We have successfully demonstrated an efficient detection of gaseous plumes from airborne LWIR hyperspectral datacubes obtained by HyperCam imager. This specific detection algorithm does not require any clear background estimation, making it ideal for airborne detection. Furthermore, since the ROC curve and the performance analysis of the detection algorithm are known [11] (at this spectral resolution of $4cm^{-1}$, and for the same sensor), we can immediately adopt the same parameters for airborne sensing. Further work should be done in order to obtain a good estimate of the quantity $T_{a(0)} \cdot \tau_a + path$ which is a critical input needed to ensure correct results. In this paper we proposed two approaches to tackle this problem that left for future work. Another enhancement method that might be available following the work in a "target mode" is using multiple images of the plume on a single pass. While the background is mainly static between two successful datacubes, the plume shape and location varies according the atmospheric turbulence and wind. This feature can be employed for an enhancement of the detection fidelity and in order to reject possible false positives.

REFERENCES

[1] Martin Chamberland ; Vincent Farley ; Alexandre Vallières ; André Villemaire ; Louis Belhumeur, et al., "High-performance field-portable imaging radiometric spectrometer technology for hyperspectral imaging applications", Proc. SPIE 5994, Chemical and Biological Sensors for Industrial and Environmental Security, 59940N (November 09, 2005).

[2] Jacob L. Harley and Kevin C. Gross, "Remote quantification of smokestack effluent mass flow rates using imaging Fourier transform spectrometry", Proc. SPIE 8018, Chemical, Biological, Radiological, Nuclear, and Explosives (CBRNE) Sensing XII, 801813 (June 03, 2011).

[3] S. M. Adler-Golden ; P. Conforti ; M. Gagnon ; P. Tremblay and Martin Chamberland, "Long-wave infrared surface reflectance spectra retrieved from Telops Hyper-Cam imagery", Proc. SPIE 9088, Algorithms and Technologies for Multispectral, Hyperspectral, and Ultraspectral Imagery XX, 90880U (June 13, 2014).

[4] Kevin C. Gross ; Chris Borel ; Allen White ; Stephen Sakai ; Rebecca DeVasher, et al., "First imaging Fourier-transform spectral measurements of detonation in an internal combustion engine", Proc. SPIE 7812, Imaging Spectrometry XV, 78120J (August 13, 2010).

[5] Wendy Hubbard ; Gary Bishop ; Jean-Philippe Gagnon ; Philippe Lagueux ; Sion Hannuna, et al., "Detection of disturbed earth using hyperspectral LWIR imaging data", Proc. SPIE 7835, Electro-Optical Remote Sensing, Photonic Technologies, and Applications IV, 78350T (October 11, 2010).

[6] Sarah E. Lane ; Leanne L. West ; Gary G. Gimmestad ; Stanislav Kireev ; William L. Smith, et al., "Hyperspectral image turbulence measurements of the atmosphere", Proc. SPIE 8355, Infrared Imaging Systems: Design, Analysis, Modeling, and Testing XXIII, 83550N (May 18, 2012).

[7] Russell E. Warren ; David B. Cohn ; Marc-André Gagnon and Vincent Farley, "Detecting liquid contamination on surfaces using hyperspectral imaging data", Proc. SPIE 9455, Chemical, Biological, Radiological, Nuclear, and Explosives (CBRNE) Sensing XVI, 94550M (May 22, 2015).

[8] Mariusz Kastek ; Tadeusz Piątkowski ; Rafal Dulski ; Martin Chamberland ; Philippe Lagueux, et al., "Multispectral and hyperspectral measurements of soldier's camouflage equipment", Proc. SPIE 8382, Active and Passive Signatures III, 83820K (May 1, 2012).

[9] E. Puckrin ; C. S. Turcotte ; P. Lahaie ; D. Dubé ; V. Farley, et al., "Airborne measurements in the infrared using FTIR-based imaging hyperspectral sensors", Proc. SPIE 7324, Atmospheric Propagation VI, 73240R (May 06, 2009).

[10] Hirsch, E., and Agassi, E., "Detection of Gaseous Plumes in IR Hyperspectral Images Using Hierarchical Clustering", Applied Optics, 46, 6368-6374, (2007).

[11] Hirsch, E., and Agassi, E., "Detection of gaseous plumes in IR hyperspectral images – performance analysis", IEEE Sensor, 10(3), 732-736, (2010).